# Solution-based single molecule imaging of surface-immobilized conjugated polymers

JACS
JOURNAL OF THE AMERICAN CHEMICAL SOCIETY

Article

pubs.acs.org/JACS

# Solution-Based Single Molecule Imaging of Surface-Immobilized Conjugated Polymers

Paul A. Dalgarno,[†,∥] Christopher A. Traina,[§] J. Carlos Penedo,[†,‡] Guillermo C. Bazan,*[,§] and Ifor D. W. Samuel*[,†]

[†]Organic Semiconductor Centre, SUPA, School of Physics and Astronomy and [‡]Biomedical Science Research Complex (BSRC), University of St. Andrews, North Haugh, St Andrews, Fife, KY16 9SS, United Kingdom

[§]Department of Materials and Chemistry and Biochemistry, Centre for Polymers and Organic Solids, University of California, Santa Barbara, California 93106, United States

Supporting Information

**ABSTRACT:** The photophysical behavior of conjugated polymers used in modern optoelectronic devices is strongly influenced by their structural dynamics and conformational heterogeneity, both of which are dependent on solvent properties. Single molecule studies of these polymer systems embedded in a host matrix have proven to be very powerful to investigate the fundamental fluorescent properties. However, such studies lack the possibility of examining the relationship between conformational dynamics and photophysical response in solution, which is the phase from which films for devices are deposited. By developing a synthetic strategy to incorporate a biotin moiety as a surface attachment point at one end of a polyalkylthiophene, we immobilize it, enabling us to make the first single molecule fluorescence measurements of conjugated polymers for long periods of time in solution. We identify fluctuation patterns in the fluorescence signal that can be rationalized in terms of photobleaching and stochastic transitions to reversible dark states. Moreover, by using the advantages of solution-based imaging, we demonstrate that the addition of oxygen scavengers improves optical stability by significantly decreasing the photobleaching rates.

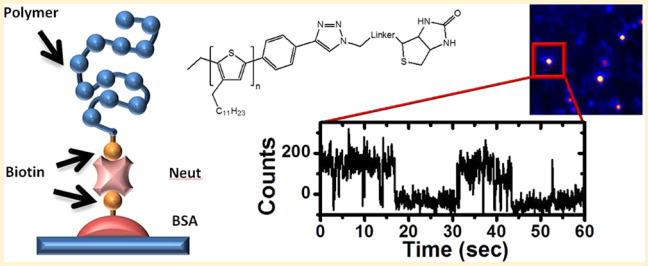


## INTRODUCTION

Conjugated polymers are the enabling materials for polymer LEDs,[1] lasers,[2] solar cells,[3,4] and field-effect transistors,[4] all of which show significant potential for modern optoelectronic technologies. Despite this commercial potential, much remains unknown about the underlying photophysical behavior of the polymers. Conjugated polymers are large, complex macromolecules in which the electronic and photophysical functions, including emission quantum yield, charge carrier mobility, spectral characteristics, and optical stability, are all intrinsically linked to polymer conformation, aggregation, and, ultimately, chromophore interaction. Moreover, given that the polymer film in the device can inherit the structural state from the processing solution,[5,6] controlling the conformation in solution is a crucial step to rationally improve device performance. Consequently, there exists a major challenge to reveal the fundamental relationship between polymer shape, conformation, and function at the single polymer level and in doing so provide an understanding of polymer behavior that will directly link to device performance.

Single molecule studies of conjugated polymers have been established in recent years[7−11] with the majority of work focusing on MEH-PPV[7−9] in addition to polyfluorenes[10] and polythiophenes.[11] Almost exclusively the established procedure is to probe single polymer chains embedded in an inert host matrix, such as PMMA or polystyrene.[12] There have been several key discoveries, such as the observation of energy funneling within the polymer to the lowest available chromophore.[7] Additional work has shown detailed vibronic structure,[13] photon antibunching,[14,15] narrow spectral line width, and nonemissive dark states[16] and revealed the potential for single polymer organic spintronics[17] along with device optimization through understanding film annealing at the molecular limit.[18−20] This wealth of information, which is unavailable with ensemble measurements, highlights the significant impact of single molecule studies for understanding conjugated polymers.

Despite the remarkable insights delivered by such techniques, host-matrix-based single molecule imaging remains limited. Highly dilute films represent only one of four defining polymer environments (bulk solution, film, isolated solution and isolated film) each of which display very different photophysical properties.[21] In each case, the functionality is defined by disorder and aggregation. Only intrachain interactions are possible in isolated environments, whereas in bulk solutions both intrachain and interchain interactions need to be considered. Solvent properties dominate conformation and

**Received:** December 5, 2012
**Published:** April 17, 2013

   dx.doi.org/10.1021/ja311874f | J. Am. Chem. Soc. 2013, 135, 7187−7193

therefore behavior, in solution. This also means that they strongly influence the properties of films that are deposited from solution. Not only can this result in difficulty in isolating single chains from small aggregates in single molecule studies[21] but also leads to the well-established relationship between solvent choice and device functionality.[5,6,22,23] Of the four defining environments, isolated chains in solution are, in principle, the most fundamental with behavior defined primarily by solvent properties and intrachain interactions. In addition it provides a uniquely dynamic environment in which polymer conformation can be directly manipulated and correlated to photophysical properties.

Solution-based single molecule imaging is unfortunately extremely challenging with no established strategy. In order to observe dynamic fluctuations a single polymer must be studied for long periods of time, requiring an effective immobilization strategy such that the backbone still preserves its conformational dynamics. Recent work on slowly diffusing MEH-PPV chains in a high viscosity, toluene solution with a low molecular weight polystyrene base approaches a possible solution.[24] However, high viscosity solvents are required, and nonspecific adsorption offers limited control over polymer immobilization. An alternative strategy has employed water-soluble MPS-PPV encapsulated in lipid vesicles.[25] However, vesicles are a closed system and are limited to aqueous environments.

We respond in this paper to these challenges by establishing a new strategy that demonstrates the proof of principle for the effective immobilization and isolation of single polymers in a fluid solution medium. We utilize end-group site-specific immobilization of conjugated polymers, specifically biotin functionalized poly(3-dodecylthiophene) (**bi-P3DDT**), to immobilize at only one end, allowing for the chain to extend freely into the solvent and adopt dynamic conformations dictated only by solvent properties. We demonstrate the ability to interrogate single polymer dynamics for extended time periods, until photobleaching (>minutes). In addition we show that by taking advantage of the flexibility of a solution-based environment, it is possible to restrict the photobleaching rate and increase the total fluorescence output from a single polymer more than 4-fold by the addition of a water compatible oxygen scavenger agent.

## RESULTS AND DISCUSSION

**Polymer Molecular Design and Synthesis.** Our strategy for solution-based imaging of conjugated polymers is based on the specific interaction between the small molecule biotin and neutravidin, which is one of the strongest noncovalent binding events known in nature, with association constants in the picomolar range. Such an interaction is commonly used in a variety of purification and analysis methods in molecular biology and when implemented at the single molecule level has provided a platform that is revolutionizing our understanding of biomolecular structure and function.[26,27] As shown in Figure 1a, biotin binds to the multivalent neutravidin protein, which in turn binds to biotinylated bovine serum albumin (BSA) adsorbed to glass or quartz surfaces, providing a single anchor point that isolates the molecule from the substrate surface. Importantly the single point of attachment allows for conformational freedom such that the polymer structure can respond to solvent-mediated environmental effects.

The experimental platform for single molecule imaging in Figure 1 imposes specific requirements for the conjugated polymeric material to be studied. The polymer should be

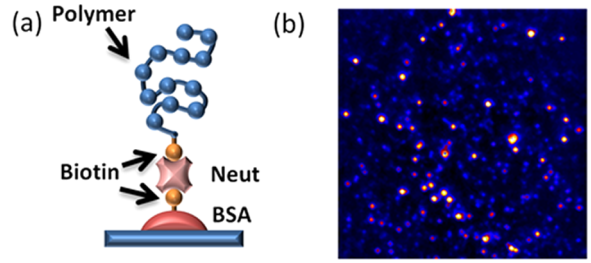


**Figure 1.** Single-molecule imaging of surface-immobilized conjugated polymers. (a) Schematic of the immobilization of a conjugated polymer chain to a substrate via biotin/neutravidin interactions. The polymer chain was designed to contain a biotin unit at a single end, bound to a single neutravidin protein in turn bound to a single BSA protein adsorbed on the glass surface. (b) Representative fluorescence image of immobilized molecules (70 × 70 $\mu$m).

strongly absorbing and sufficiently emissive with a well-defined structure and low polydispersity (PDI). Furthermore, only one chain end should be biotinylated, while the other chain end must remain unattached to permit extension of the chain into the solvent. We therefore selected an end-functionalized poly(3-alkylthiophene) material as a target. Synthetic protocols have been developed to prepare well-defined poly(3-alkylthiophene)s in a controlled manner by chain-growth Kumada catalyst-transfer polycondensation procedures.[28,29] These nickel-catalyzed methods give rise to low-polydispersity, regioregular materials with tunable average molecular weights that can be modulated via the initial catalyst to monomer ratio. Additionally, selection of an appropriate catalyst/initiator allows for controlled introduction of a functional group onto a single chain end. For example, it has been demonstrated that a catalyst/initiator of the type $L_2Ni(Br)Ar$, where L is a phosphine ligand and Ar is an aryl group, can initiate the polymerization by transfer of the aryl group to the active thiophene monomer.[30−34] A substituted aryl ring, such as a 4-(triisopropylsilylethynyl)phenyl group, would offer a reactive handle for postpolymerization functionalization by click chemistry after deprotection to the active acetylene functionality.[35,36] Thus, as shown in eq 1, where TIPS corresponds to

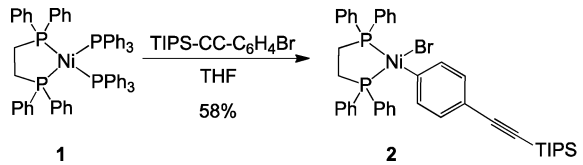


triisopropylsilyl, the catalyst/initiator **2** was synthesized from the mixed phosphine nickel complex **1** by oxidative addition of 1-bromo-4-(triisopropylsilylethynyl)benzene.[37] In this reaction, the aryl bromide was treated with a THF solution of **1** and allowed to stir for 44 h, after which time the solvent was removed. The residue was then taken up in toluene and precipitated with pentane to give TIPS-ethynyl containing **2**. The $^1$H NMR spectrum of **2** is consistent with the proposed structure, showing methyl and methine signals arising from the TIPS protecting group at 1.22 and 1.15 ppm, respectively. Two resonances in the $^{31}$P NMR spectrum at 58 and 39 ppm indicate the presence of two distinct phosphorus environments, reflecting the asymmetric nature of the complex.

Complex **2** was thus used to prepare the target biotin-terminated poly(3-dodecylthiophene), as depicted in Scheme 1. First, a THF solution of the dibromothiophene **3** was treated


dx.doi.org/10.1021/ja311874f | J. Am. Chem. Soc. 2013, 135, 7187−7193

**Scheme 1. Synthetic Entry into the End-Group Biotinylated Polythiophene Bi−P3DTT**

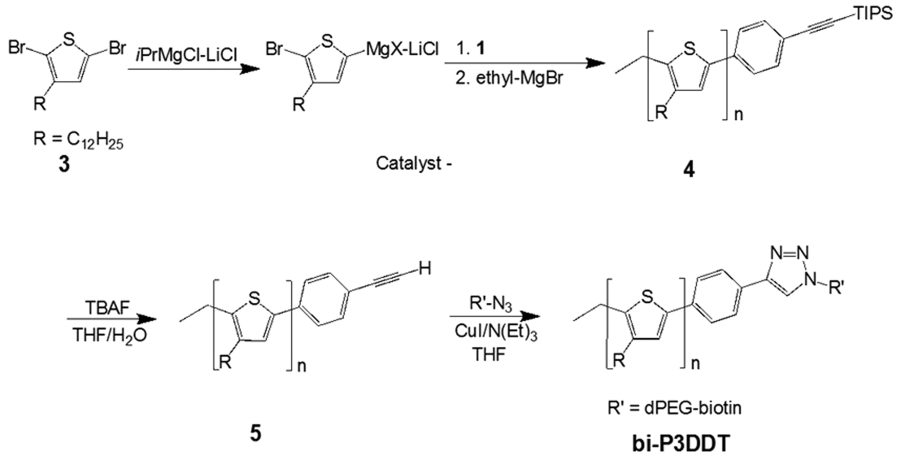


with isopropylmagnesium chloride−lithium chloride complex to give the monobromo, monomagnesio reactive monomer, and this solution was quickly added to the polymerization initiator **2**, at a monomer:initiator ratio of 100:1. After 5 min of reaction time, the polymerization was terminated with ethylmagnesium bromide to give TIPS-ethynyl-phenyl end-functionalized poly(3-dodecylthiophene) (**4**). The resulting polymer was characterized by gel permeation chromatography (GPC) using a mobile phase of $CHCl_3$ + 0.25% triethylamine, which gave a number average molecular weight ($M_n$) of 19 kDa, which would correspond at face value to ∼75 repeat units and a PDI of 1.4, as estimated relative to poly(styrene) standards. It is worth noting here that the $M_n$ values of conjugated polymers obtained by GPC are often overestimated when calculated against poly(styrene) due to the large differences in hydrodynamic volume between the two types of polymers. The $^1$H NMR spectrum of **4** is dominated by the methylene protons of the dodecyl side chain, which appear between 2.90 and 1.35 ppm, and the terminal methyl signal at 0.95 ppm. Resonances due to the aromatic thiophene protons are visible at 7.19 ppm. The $^1$H NMR spectrum also displays a small doublet at 1.25 ppm, which has been assigned to the methyl groups of the triisopropylsilyl-ethynyl group, indicating successful end group incorporation. The signal at 1.75 ppm represents protons from one methylene group of the thiophene dodecyl side chain and for each unit represents 2 protons. A comparison of the integrated intensity from the methylene resonance at 1.75 ppm and the TIPS signal at 1.25 ppm gives a ratio of 2H:0.35H, which corresponds to approximately one TIPS-ethynyl end group per 51 thiophene repeat units. This ratio of one reactive end group per 51 repeat units is lower than the initial monomer to initiator ratio used during polymerization. However, upon further investigation, this difference is not surprising. It has been shown that activation of the 2,5-dibromo-3-alkyl thiophene premonomer with organomagnesium compounds results in a 4:1 mixture of reactive vs nonreactive monomers, depending on magnesium insertion at the 5- or 2-position of the thiophene. Furthermore, the polymerization was terminated with ethylmagnesium bromide after 5 min polymerization time so as to ensure polymer end-capping with an inert alkyl group. It is likely that some unreacted monomer remained in solution at the time the polymerization was quenched.

Incorporation of the biotin functionality begins with deprotection of the ethynyl group by using tetrabutylammonium fluoride (TBAF) in THF with several drops of water as the proton source, to yield polymer **5**. The course of the deprotection reaction was followed by monitoring the disappearance of the TIPS protons at 1.25 ppm, resulting in an end-functionalized polymer which was active for copper-catalyzed azide−alkyne cycloaddition reactions. The biotin functionality was thus introduced by treatment of **5** with biotin-$dPEG_{3+4}$-azide (azide-containing biotin molecule) under click reaction conditions of CuI/triethylamine in THF to give **bi-P3DDT**. $^1$H NMR spectroscopy is unable to confirm biotin attachment, as the spectrum for **bi-P3DDT** is very similar to that of precursor **5**, with signals due to the biotin group likely overlapping with the more intense peaks of the thiophene repeat units. Therefore, FTIR spectroscopy is used to confirm the presence of the biotin functional group; bands at 1700 and 1650 $cm^{-1}$ in the IR spectrum of **bi-P3DDT**, which correspond to carbonyl groups in the biotin molecule and linker, are not present in the spectra of precursor **5**.

The terminal biotin of **bi-P3DDT** was then probed for surface immobilization reactivity. Streptavidin-coated agarose beads were treated with a THF solution of **bi-P3DDT**, and after 2 h incubation time, the beads were collected and washed to remove nonbound polymer. The **bi-P3DDT** treated beads showed strong orange luminescence under UV (365 nm) illumination, indicating biotin-mediated surface binding of **bi-P3DDT** to the steptavidin present on the beads. A control experiment conducted in a similar way but with a poly(3-dodecylthiophene), which did not contain a terminal biotin, yielded beads with negligible luminescence. Thus, the presence of a terminal biotin moiety was confirmed, and moreover, this functional group proved effective for immobilizing the polymer, as required for single molecule experiments.

**Spectral Characteristics of bi-P3DDT.** To demonstrate the principle of our solution-based immobilization methodology, we chose to immobilize **bi-P3DDT** from a 90:10 (v/v) solution of aqueous buffer (pH 7.5) and tetrahydrofuran (THF) and to image in a 100% buffer solution. **Bi-P3DDT** is soluble in THF which is fully water miscible. A 90:10 (v/v) mixture of aqueous buffer:THF was chosen for several reasons: First, the poor solvent properties of this mixture will be expected to predominantly induce a well-known collapsed coil conformation.[38] Second, as proof-of-principle for solution-based single molecule studies, the change in refractive index between the quartz surface and the aqueous medium is adequate to use wide-field total-internal reflection (TIR) as the single molecule imaging method. This improves the signal-to-


dx.doi.org/10.1021/ja311874f | J. Am. Chem. Soc. 2013, 135, 7187−7193

noise ratio compared to conventional illumination methods and, at the same time, allows us to obtain a much higher statistical characterization of polymer behavior compared to, for example, confocal methods. Lastly, an aqueous-based medium offers the possibility of exploring the effect of oxygen scavenger systems on single polymer photostability. Although, oxygen scavengers based on in situ glucose oxidation are highly effective and widely used in aqueous solution to inhibit photobleaching in organic chromophores, to date, their effect on single conjugated polymers has never been reported.

To verify the optical behavior of **bi-P3DDT** in our immobilization medium, Figure 2 shows the absorption (Figure 2a) and fluorescence (Figure 2b) of a bulk solution of **bi-P3DDT** in pure THF and 90:10 buffer:THF solution. Bulk solutions were prepared with a saturated **bi-P3DDT** THF solution (<0.33 mg/mL), stirred for 4 h, and filtered through a 1.45 $\mu$m filter. For bulk spectroscopy measurements, this stock was further diluted by a factor of 10 either in pure THF or aqueous buffer. In the aqueous buffer there is a significant red-shift ( ~100 nm) for both absorption and emission accompanied by a reduction in fluorescence intensity and the appearance of two distinct peaks at 650 and 725 nm. These spectral signatures suggest collapsed and aggregated chains, a phenomenon that was also observed for poly(3-dodecylthiophene) in poor solvent mixtures.[38] Single molecule fluorescence was excited at 532 nm and collected over the complete bandwidth of the bulk fluorescence emission by collecting all fluorescence above 550 nm.

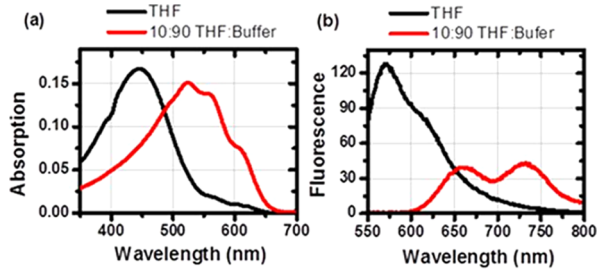


**Figure 2.** Absorption (a) and fluorescence emission spectra (b) obtained for **bi-P3DDT** in THF (black) and 10:90 THF:aqueous buffer (red) solutions. Fluorescence spectra were collected at 532 nm excitation wavelength.

**Single Molecule Imaging.** To prepare individual polymers for single molecule immobilization, a solution of **bi-P3DDT** in THF was prepared as described in the previous section. This stock solution was then diluted 100 times in THF and further stirred for 4−5 h. This final solution was diluted 10 times in the buffer medium before being incubated on a BSA-neutravidin precoated microchannel. After 15 min the channel was thoroughly rinsed with fresh buffer and the sample was ready for imaging. In aqueous medium the channel is robust against leakage and evaporation for several hours, and molecular imaging from the same channel is reported for periods of time in excess of 5 h. Additionally the channel is robust against any form of contamination from channel breakdown, which dominates when imaging is attempted in pure organic solvents. The configuration is such that replacement of the imaging medium is possible at any time during the experiment, allowing for directly comparative experiments under different environmental conditions.

SM TIRF microscopy was performed at varying incident powers, defined as the estimated power density at the interface between the quartz slide and the solution medium, from 0.015 to 0.74 W/cm$^2$. Images were collected in custom built relay optics with a 550 nm long pass filter and an emCCD camera (Andor, Belfast). Figure 1b shows that our immobilization protocol produced ~200−400 isolated, bright spots spatially distinct on the emCCD field of view. We report correlated concentration-dependent changes in the number of spots and distinct single step bleaching and blinking events, see below, providing confidence we are observing, at least in part, individual polymer chains or small aggregates. To confirm that the observed spots are due to specific immobilization of the biotinilated polymer onto the BSA-neutravidin-coated quartz surface and not caused by nonspecific adsorption, we performed control experiments using both uncoated and BSA-only functionalized surfaces, Figure S1. Under both of these conditions, for the same incubation period and with sample concentrations up to 10 times those described above, we report no immobilized molecules. We are therefore confident we are observing single immobilized P3DDT molecules imaged in solution.

**Oxygen-Dependent Photostabilization.** We first investigated polymer photostability by taking advantage of the significant degree of flexibility that solution-based imaging allows in modifying the environment of the molecules. One of the most significant impacts for biomolecular imaging has been the use of oxygen scavengers to significantly reduce photobleaching.[26] We use the common oxygen scavenger imaging buffer, glucose oxidase, 165 U/ml and catalase, 2170 U/ml in a 6% glucose/buffer solution. Figure 3 shows the normalized time-dependent variation in the fluorescence signal as a function of excitation power in the absence (Figure 3a) and presence (Figure 3b) of oxygen scavenger imaging buffer. The observed fluorescence trajectory at each excitation power is the result of adding together the individual trajectories of more than 1000 molecules. Over two decades of excitation power there is between a 4- and 10-fold stabilization of the fluorescence in the presence of oxygen scavenger, quantified in Figure 3c by plotting the longer lifetime component of a

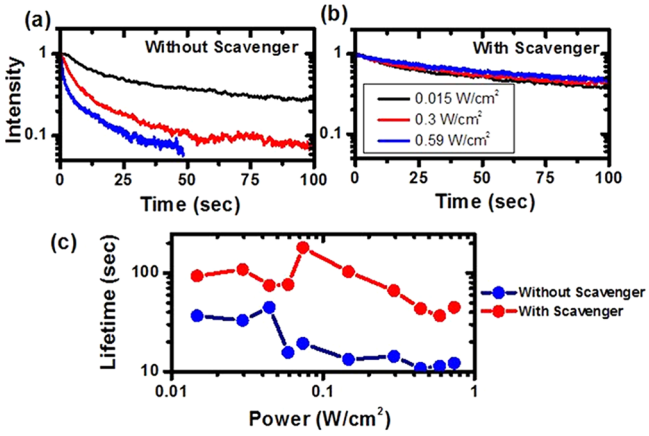


**Figure 3.** Effect of oxygen scavenger on polymer photostability. The normalized sum of intensity traces from 1200 individual molecules as a function of excitation power is shown (a) without and (b) with scavenging buffer. (c) Fitted photobleaching lifetimes as a function of power from data shown in (a) and (b).


dx.doi.org/10.1021/ja311874f | J. Am. Chem. Soc. 2013, 135, 7187−7193

biexponential fit to equivalent data from Figure 3a,b at 10 different excitation powers. Although each decay is biexponential (Figure S2), they are all dominated by the longer lifetime component which we attribute to the photobleaching dynamics.[39] Full analysis of the photobleaching lifetimes, the short and long lifetime contributions and stabilization are shown in Figure S2. We therefore demonstrate that oxygen scavenging is a viable avenue for photostabilization of conjugated polymers. Importantly this stabilization allows us to reduce photobleaching and therefore make clear measurements of the distinct molecular behavior from each molecule. No further stabilization of the fluorescence emission, including removal of transiently populated dark states (blinking), was observed when adding triplet-state quenchers, such as Trolox (derivative of vitamin E) or $\beta$-mercaptoethanol.

**Single Molecule Behavior.** We now categorize molecular behavior into distinct patterns by inspection of the individual fluorescence trajectories. In all data sets, at all excitation powers and for both with and without oxygen scavengers, we consistently identify four main trace types. Examples of three of these fluorescence types are shown in Figure 4. The

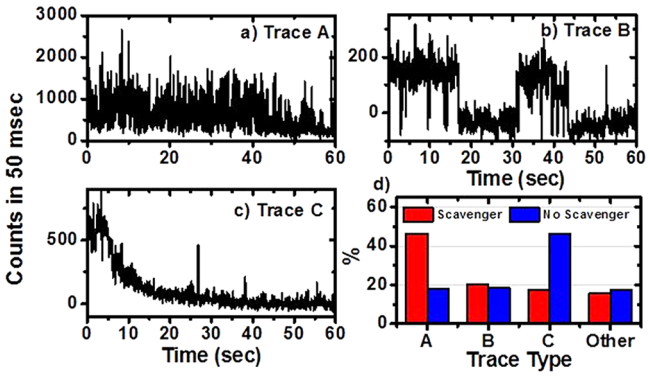


**Figure 4.** (a–c) Representative trajectories of the single molecule fluorescence patterns observed for **bi-P3DDT** in aqueous medium. Only trajectories in the presence of oxygen scavenger buffer are shown. Trajectories were obtained with 0.59 W/cm$^2$ incident excitation power and with 50 ms integration rate. (d) Statistical distribution of single molecule fluorescence patterns in the presence (red) and absence of oxygen scavenging additives (blue).

classification of the observed fluorescence traces was carried out following a number of criteria based on intensity, level of dynamic fluctuation, presence of discrete fluorescence states and photobleaching. The specific patterns can be described as follows: (A) rapid fluctuations (millisecond time scale) between two or more highly emissive states occasionally interlaced with transitions to dark states lasting several seconds; (B) trajectories dominated by fluctuations between a low emitting state and a dark state both lasting for several seconds, reminiscent of blinking transitions to triplet states commonly observed in single chromophore organic dyes; (C) trajectories showing a highly emissive state exponentially decaying to background level, similar to that observed in highly aggregated systems; and (D) the fourth classification "other", which is not shown, corresponds to a wide variety of trace types that show no easily classified behavior.

For the three main classes we do not observe the complex, multileveled photoblinking dynamics reported from collapsed MEH-PPV chains cast from poor solvent.[9] Nor do we observe the two state blinking behavior over a constant bleaching background of MEH-PPV in high viscosity solvent.[24] Nonreversible photobleaching is prominent for all trace types, but when oxygen scavenger is present, emission can be stabilized for many minutes, even at high excitation power.

Figure 4d shows the statistical distribution of single molecule fluorescence behavior in the presence and absence of oxygen scavenger classified following the criteria described previously. In the presence of oxygen scavengers, a total of 1200 molecules, taken evenly from data at 0.015, 0.3, and 0.59 W/cm$^2$, were analyzed. The relative ratio of trace types is, to within 5%, consistent between excitation powers, Figure S3. Molecular behavior is dominated by trace type A, 45%, with bright rapidly unresolved fluctuations with little or no characteristic single molecule blinking. There is an even distribution (20%) of trace types B and C. For data without oxygen scavengers, where 550 molecules are analyzed, (Figure 4d, blue) molecular behavior is dominated (50%) by exponential decays, with roughly 20% of types A and B.

The molecular classifications reveal a number of interesting points: First, there is a notable contribution, 20%, of traces that show distinct, single step blinking or bleaching events, trace type B. This behavior is typical for collapsed, single chains cast from bad solvents[7,40,41] and can be attributed to energy funneling to the lowest-energy chromophore or Förster transfer induced photogenerated quenching.[42] Second, there is a lack of clear multilevel blinking from any molecules, often seen in MEH-PPV. This could be attributed to very few active chromophores, to chain quenching as discussed above[42] or to nonemissive dark states.[16] Third, there is a range of distinct molecular behaviors for identical environmental conditions of which the statistics remain unchanged over two decades of excitation power, Figure S3. Fourth, oxygen scavenging shifts the dominated trace type from exponential decays without scavenger (type C) to rich transient dynamics with scavenger (type A), without affecting the proportion of single step blinking/bleaching traces.

The final two points suggest a complex conformational landscape of the molecules under study. The bad solvent environment is expected to induce collapsed chains, Figure 2, which in principle should give rise to single step blinking and bleaching events remnant of trace type B.[7,39,40] However only 20% of traces demonstrate such behavior. The majority show behavior expected from a multichromophoric system. In the absence of oxygen scavenger this manifests itself as that of an exponentially decreasing intensity produced by the gradual photobleaching of multiple chromophores. With scavenger, bleaching is removed, and the dynamics in trace type A suggest continuous emission from multiple emitters each with differing blinking and intensity dynamics. However, this is clearly an oversimplification. Our proof of principle experiment limits further investigation, but we tentatively conclude that we are observing behavior from two classes of molecular states. One class is stable, tightly collapsed single chains with clear, single step blinking dynamics dominated by efficient energy funneling or quenching behavior (type B). The other class is either small aggregates of multiple emitters or dynamic, collapsed chains undergoing constant conformational restructuring which prevents funneling/quenching behavior (mostly types A and C depending on the environment).

**Autocorrelation Analysis.** To investigate in further detail the dynamics, we calculated the autocorrelation function of representative fluorescence trajectories corresponding to the dynamic groups A and B. This analysis is commonly used to


dx.doi.org/10.1021/ja311874f | J. Am. Chem. Soc. 2013, 135, 7187–7193

extract the underlying hidden dynamics in fast fluctuating systems providing a global macroscopic rate constant that groups the sum of the forward and backward interconversion rates.[43] We observe similar autocorrelation dynamics between group types A and B (see Figure S4) and therefore group the autocorrelation results as a single set, Figure 5. The

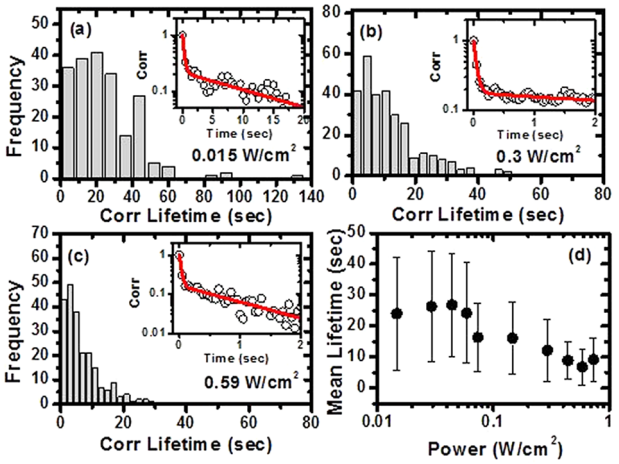


**Figure 5.** Autocorrelation analysis of trace classification. (a–c) Histogram of the fitted lifetime of the correlation function $G(t)$ from data at 0.015, 0.3, and 0.59 W/cm$^2$ with oxygen scavenger. Insets show a single example $G(t)$ with biexponential fit. (d) The mean slow component correlation lifetime from between 100 and 300 molecules at each power, with std dev, as a function of excitation power.

autocorrelation function of each trace fitted well to a biexponential decay with a minor component lifetime of ~200 ms and a dominant slow component with a lifetime >5s. Our primary result is that the mean of the slow component lifetime, averaged over 100–300 molecules at each excitation power, was dependent on the excitation intensity (Figure 5d) and showed a 2–3 fold decrease with increasing excitation power. On the other hand, the mean of the fast component reflected dynamic events taking place close to our frame rate at all excitation powers, Figure S7. These findings provide evidence for the polymer exhibiting molecular processes at two very different dynamic regimes. Although this is an oversimplification and the nature of these processes will need further investigation, we can still extract some conclusions.

First, our collection bandpass above 550 nm collects virtually all of the polymer emission range, Figure 2, thus, the observed intensity fluctuations are unlikely to be due to spectral diffusion. Second, the discrete jumps between different emissive states (type A) or between emissive and dark states (type B) suggest a certain degree of cooperativity between conjugated regions of the polymer as suggested for other organic polymers including MEH-PPV and dPPV-PPyV.[43] Third, the lack of multilevel blinking and bleaching events suggests a more homogeneous distribution of dynamic states for **bi-P3DDT** in solution over host matrix environments. Fourth, the power dependence of the slow component suggests an underlying photoblinking mechanism responsible for the rapid transient dynamics. Overall, the observation of a major population of fluorescence trajectories in the presence of oxygen scavenger showing fast dynamic exchange between highly emissive states in **bi-P3DDT** and taking place in ~200 ms time scale, as reflected by the fast component of the autocorrelation function, points toward the polymer structure dynamically sampling different packing conformations, each of them having different quantum yields. Indeed, NMR and photophysical studies of MEH-PPV morphology in low-quality solvents indicate that microscopic variations in the degree of polymer packing may account for up to two-thirds of variation in quantum efficiency.[23]

## CONCLUSION

To summarize, we have demonstrated single molecule spectroscopy of immobilized single polymer chains in solution. A novel type of conjugated polymer, namely **bi-P3DDT**, has been designed that contains the biotin structural element for selective end-group binding to neutravidin-modified substrates. The synthesis involves a controlled polymerization reaction with an initiator that imparts a masked acetylene functional group. The latter can serve for straightforward incorporation of various functionalities by reaction with substituted azides and provides a flexible platform for further derivatization. **Bi-P3DDT** can form the foundation for solution-based single molecule imaging of site-specific immobilized polymers while, in principle, retaining conformational freedom to be dictated by solvent. As an example we have demonstrated this technique with **bi-P3DDT** in a 90:10 aqueous:THF solution. In addition to demonstrating photostabilization through the use of standard oxygen scavenging, we observe largely heterogenic behaviors separated into only two distinct classes: one showing distinct single step blinking and bleaching and the other displaying rapid intensity fluctuations resembling multiple emitters. We demonstrated the principle in an intentionally bad solvent, limiting molecular confirmation to tightly collapsed chains. However, the methodology is compatible with confocal imaging in organic solvents and can be combined with click chemistry to covalently link the polymer to the surface thus removing the need for immobilization protein.

## ASSOCIATED CONTENT

### Supporting Information

Confirmation of immobilization strategy; analysis of photobleaching lifetimes in the presence and absence of oxygen scavengers; classification of single molecule intensity trajectories as a function of excitation power; trace dependent autocorrelation analysis; statistics of autocorrelation lifetimes; fast correlation component and frame rate; materials; and methods. This material is available free of charge via the Internet at http://pubs.acs.org.

## AUTHOR INFORMATION

### Corresponding Author

idws@st-andrews.ac.uk; bazan@chem.ucsb.edu

### Present Address

[‖]Institute of Biological Chemistry, Biophysics and Bioengineering, School of Engineering and Physical Sciences, Heriot-Watt University, Edinburgh, EH14 4AS, United Kingdom.

### Notes

The authors declare no competing financial interest.

## ACKNOWLEDGMENTS

St Andrews acknowledges support from the Scottish University Physics Alliance (SUPA) and funding from EPSRC (grant no. EP/G061688/1). UCSB acknowledges funding from NSF (grant DMR 103548).

## REFERENCES


(1) Grimsdale, A. C.; Chan, K. L.; Martin, R. E.; Jokisz, P. G.; Holmes, A. B. *Chem. Rev.* **2009**, *109*, 897.
(2) Samuel, I. D. W.; Turnbull, G. A. *Chem. Rev.* **2007**, *107*, 1272.
(3) Kim, Y.; Cook, S.; Tuladhar, S. M.; Choulis, S. A.; Nelson, J.; Durrant, J. R.; Bradley, D. D. C.; Giles, M.; McCulloch, I.; Ha, C. S.; Ree, M. *Nat. Mater.* **2006**, *5*, 197.
(4) Facchetti, A. *Chem. Mater.* **2011**, *23*, 733.
(5) Nguyen, T. Q.; Kwong, R. C.; Thompson, M. E.; Schwartz, B. J. *Appl. Phys. Lett.* **2000**, *76*, 2454.
(6) Shaheen, S. E.; Brabec, C. J.; Sariciftci, N. S.; Padinger, F.; Fromherz, T.; Hummelen, J. C. *Appl. Phys. Lett.* **2001**, *78*, 841.
(7) Barbara, P. F.; Gesquiere, A. J.; Park, S. J.; Lee, Y. J. *Acc. Chem. Res.* **2005**, *38*, 602.
(8) Kobayashi, H.; Onda, S.; Furumaki, S.; Habuchi, S.; Vacha, M. *Chem. Phys. Lett.* **2012**, *528*, 1.
(9) Lupton, J. M. *Adv. Mater.* **2010**, *22*, 1689.
(10) Schindler, F.; Lupton, J. M. *Nano Lett.* **2010**, *10*, 2683.
(11) Khalil, G. E.; Adawi, A. M.; Fox, A. M.; Iraqi, A.; Lidzey, D. G. *J. Chem. Phys.* **2009**, *130*, 044903.
(12) Yu, J.; Hu, D.; Barbara, P. F. *Science* **2000**, *289*, 1327.
(13) Muller, J. G.; Anni, M.; Scherf, U.; Lupton, J. M.; Feldmann, J. *Phys. Rev. B* **2004**, 70.
(14) Hollars, C. W.; Lane, S. M.; Huser, T. *Chem. Phys. Lett.* **2003**, *370*, 393.
(15) Kumar, P.; Lee, T.-H.; Mehta, A.; Sumpter, B. G.; Dickson, R. M.; Barnes, M. D. *J. Am. Chem. Soc.* **2004**, *126*, 3376.
(16) Lin, H.; Tian, Y.; Zapadka, K.; Persson, G.; Thomsson, D.; Mirzov, O.; Larsson, P.-O.; Widengren, J.; Scheblykin, I. G. *Nano Lett.* **2009**, *9*, 4456.
(17) Lupton, J. M.; McCamey, D. R.; Boehme, C. *ChemPhysChem* **2010**, *11*, 3040.
(18) Vogelsang, J.; Adachi, T.; Brazard, J.; Bout, D. A. V.; Barbara, P. F. *Nat. Mater.* **2011**, *10*, 942.
(19) Vogelsang, J.; Brazard, J.; Adachi, T.; Bolinger, J. C.; Barbara, P. F. *Angew. Chem., Int. Ed.* **2011**, *50*, 2257.
(20) Bolinger, J. C.; Traub, M. C.; Brazard, J.; Adachi, T.; Barbara, P. F.; Vanden Bout, D. A. *Acc. Chem. Res.* **2012**, *45*, 1992.
(21) Lin, H.; Hania, R. P.; Bloem, R.; Mirzov, O.; Thomsson, D.; Scheblykin, I. G. *Phys. Chem. Chem. Phys.* **2010**.
(22) Samuel, I. D. W.; Rumbles, G.; Collison, C. J.; Moratti, S. C.; Holmes, A. B. *Chem. Phys.* **1998**, *227*, 75.
(23) Collison, C. J.; Rothberg, L. J.; Treemaneekarn, V.; Li, Y. *Macromolecules* **2001**, *34*, 2346.
(24) Onda, S.; Kobayashi, H.; Hatano, T.; Furumaki, S.; Habuchi, S.; Vacha, M. *J. Phys. Chem. Lett.* **2011**, *2*, 2827.
(25) Karam, P.; Ngo, A. T.; Rouiller, I.; Cosa, G. *Proc. Natl. Acad. Sci. U.S.A.* **2010**, *107*, 17480.
(26) Roy, R.; Hohng, S.; Ha, T. *Nat. Methods* **2008**, *5*, 507.
(27) Zhuang, X. W.; Bartley, L. E.; Babcock, H. P.; Russell, R.; Ha, T. J.; Herschlag, D.; Chu, S. *Science* **2000**, *288*, 2048.
(28) Chen, T. A.; Rieke, R. D. *J. Am. Chem. Soc.* **1992**, *114*, 10087.
(29) McCullough, R. D.; Lowe, R. D. *J. Chem. Soc., Chem. Commun.* **1992**, 70.
(30) Beryozkina, T.; Senkovskyy, V.; Kaul, E.; Kiriy, A. *Macromolecules* **2008**, *41*, 7817.
(31) Bronstein, H. A.; Luscombe, C. K. *J. Am. Chem. Soc.* **2009**, *131*, 12894.
(32) Senkovskyy, V.; Sommer, M.; Tkachov, R.; Komber, H.; Huck, W. T. S.; Kiriy, A. *Macromolecules* **2010**, *43*, 10157.
(33) Senkovskyy, V.; Tkachov, R.; Beryozkina, T.; Komber, H.; Oertel, U.; Horecha, M.; Bocharova, V.; Stamm, M.; Gevorgyan, S. A.; Krebs, F. C.; Kiriy, A. *J. Am. Chem. Soc.* **2009**, *131*, 16445.
(34) Tkachov, R.; Senkovskyy, V.; Komber, H.; Sommer, J.-U.; Kiriy, A. *J. Am. Chem. Soc.* **2010**, *132*, 7803.
(35) Smeets, A.; Van den Bergh, K.; De Winter, J.; Gerbaux, P.; Verbiest, T.; Koeckelberghs, G. *Macromolecules* **2009**, *42*, 7638.
(36) Smeets, A.; Willot, P.; De Winter, J.; Gerbaux, P.; Verbiest, T.; Koeckelberghs, G. *Macromolecules* **2011**, *44*, 6017.
(37) Traina, C. A.; Bakus, R. C., II; Bazan, G. C. *J. Am. Chem. Soc.* **2011**, *133*, 12600.
(38) Rumbles, G.; Samuel, I. D. W.; Magnani, L.; Murray, K. A.; DeMello, A. J.; Crystall, B.; Moratti, S. C.; Stone, B. M.; Holmes, A. B.; Friend, R. H. *Synth. Met.* **1996**, *76*, 47.
(39) Gensch, T.; Böhmer, M.; Aramendía, P. F. *J. Phys. Chem. A* **2005**, *109*, 6652.
(40) Ebihara, Y.; Vacha, M. *J. Phys. Chem. B* **2008**, *112*, 12575.
(41) Huser, T.; Yan, M.; Rothberg, L. J. *Proc. Natl. Acad. Sci. U.S.A.* **2000**, *97*, 11187.
(42) Mirzov, O.; Cichos, F.; von Borczyskowski, C.; Scheblykin, I. G. *Chem. Phys. Lett.* **2004**, *386*, 286.
(43) Yip, W.-T.; Hu, D.; Yu, J.; Vanden Bout, D. A.; Barbara, P. F. *J. Phys. Chem. A* **1998**, *102*, 7564.